

Seismic landslide analysis: Gurpinar (Istanbul) as a case history

Ferhat Ozcep · Engin Erol · Fatih Saraçoğlu ·
Mustafa Haliloğlu

Received: 5 April 2010 / Accepted: 2 November 2010 / Published online: 20 November 2010
© Springer-Verlag 2010

Abstract Slope failures triggered by earthquakes are among the most important soil mechanics problems. In this study, static and pseudostatic analyses of slope stability for earthquake conditions were carried out in the Gurpinar area. In situ testing (SPT) was carried out and laboratory samples were obtained from six boreholes (maximum depth 50.0 m) to determine soil classification and strength characteristics. Geophysical studies (seismic refraction and MASW) were also carried out in the area to estimate the structure and stiffness strength characteristics of the slope to 50.0 m depth. All field and laboratory data were used to determine the mechanical and structural (geometrical) behavior of the slope. In order to solve the slope stability problem, three soil slope models were considered. Pseudostatic analysis was carried out to estimate the earthquake acceleration seismic hazard in the region. These analyses showed that, while there was no potential slope instability under static load conditions, some problems would appear with increasing earthquake acceleration. A geotechnical slope improvement project is proposed for the study area.

Keywords Seismic slope stability · Earthquakes · Gurpinar (Istanbul)

Introduction

Slope instability is responsible for damage to public and private property every year. Slope failures can be manifested as landslides or by slower processes such as soil creep. Buildings and infrastructure located on or in the path of a landslide can be seriously damaged or destroyed. Slope instability is a complex phenomenon that can occur at many scales and for many reasons. Slope stability analyses and stabilization require an understanding and evaluation of the processes that govern the behavior of slopes. Examples of triggering mechanisms or agitation factors of slopes include earthquakes, water, slope angle, and slope strength characteristics.

The essential geological, hydrological and seismological properties of a slope must be understood as well as the methods for obtaining the necessary input data for reliable slope stability analyses. Scientists and engineers utilize many tools to investigate all aspects of slope instability. Key factors in slope stability investigation include determining the boundaries of the slope instability, establishing a history of previous slope movement, assessing landslide cause, modeling landslide initiation and the travel paths taken by moving landslide debris, assessing the damage to affected buildings and structures, and preparing recommendations for stabilizing slopes.

Primarily, slope failure is related to the following:

- soil properties or soil type of slope,
- geometry of slope,
- weight,
- water content (one of the most aggressive factors),

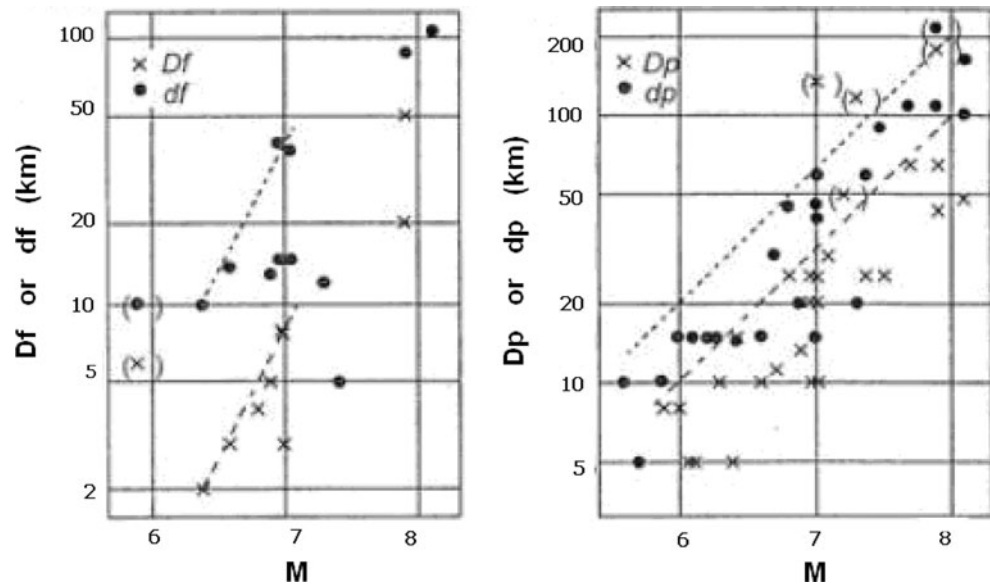
F. Ozcep (✉)
Department of Geophysical Engineering,
Faculty of Engineering, Istanbul University, Istanbul, Turkey
e-mail: ferozcep@istanbul.edu.tr

E. Erol
Granit Jeofizik, Catalca, Istanbul, Turkey

F. Saraçoğlu
SRC Geoteknik ve Deprem Mühendisliği, Istanbul, Turkey

M. Haliloğlu
Jeoson Yeraltı Araştırma ve İnşaat Merkezi, Istanbul, Turkey

Fig. 1 Relationship between magnitude and distance to slope failure in Japan (Tamura 1978; ISSMFE 1993)



- shear strength reduction in the slope,
- * tension cracks,
- * vibrations and earthquakes.

Estimation of earthquake risk in city planning is one of the most important tasks in avoiding natural disasters. Seismic risk evaluation includes the vulnerability of the value at risk and the hazard. Slope instability generated by seismic events was investigated in the present study. Several studies on seismic slope stability analysis have been reported (Matasovic 1991; Bourdeau et al. 2004; Cherubini et al. 2004).

The main goal of the research carried out in Gurpinar (Istanbul) as a case study was to evaluate current techniques of static and seismic slope analysis and mitigation of earthquake-induced landslides produced by seismically induced ground deformations.

Earthquakes and slope failures

Earthquakes and related slope failures in Japan were investigated by Tamura (1978); in Fig. 1, D_f is the distance from a fault to the outer boundary of the zone where many slope failures have occurred; d_f is the distance from a fault to the outer boundary of the zone where few slope failures have occurred; D_p is the distance from an earthquake epicenter to the outer boundary of the zone where many slope failures have occurred; and d_p is the distance from an earthquake epicenter to the outer boundary of the zone where few slope failures have occurred.

In the Manual for Zonation on Seismic Geotechnical Hazards (prepared by the Technical Committee for Earthquake Geotechnical Engineering, TC4, of the International

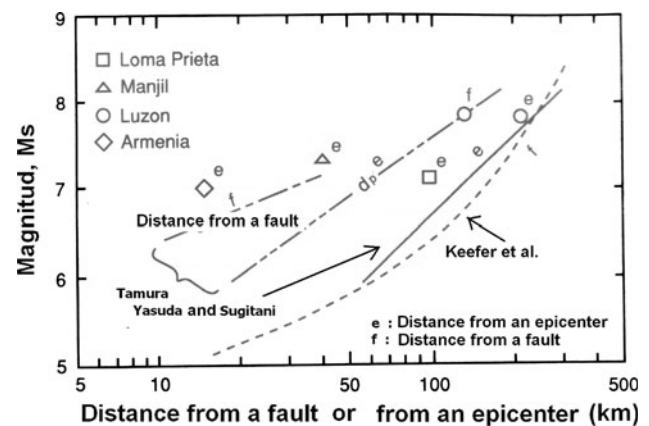


Fig. 2 Comparison of relationships between magnitude and maximum distance from a fault or an epicenter (ISSMFE 1993)

Society for Soil Mechanics and Geotechnical Engineering), the magnitude–distance criteria and historic information are summarized in Figs. 2 and 3.

The curves shown in Fig. 4, giving maximum epicentral distance for slope failure as a function of magnitude, are recommended by ISSMFE (1993) for use in microzoning.

Slope stability evaluation methods

Slope stability evaluation methods may be categorized as static and seismic methods.

Slices method (static load state) for effective soil pressure

The factor of safety (FS) for slope stability with undrained shear strength parameters ϕ' , c' are given by:

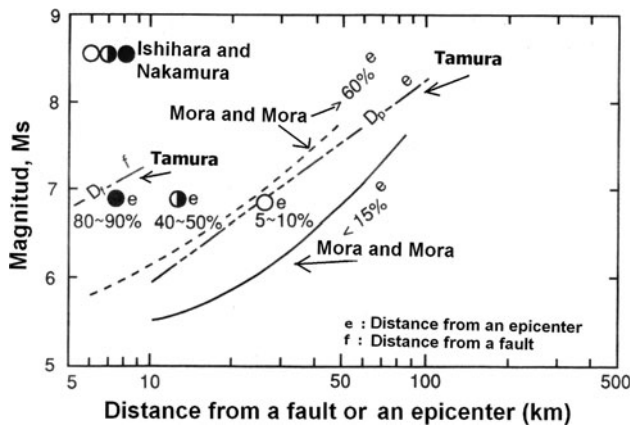


Fig. 3 Comparison of relationships between magnitude and distance from a fault or an epicenter causing different percentage of slope failures (ISSMFE 1993)

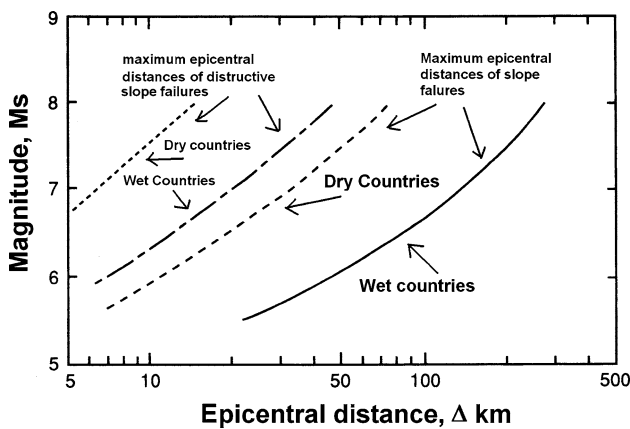


Fig. 4 General relationships between magnitude and the epicentral distance of slope failures (ISSMFE 1993)

$$FS = \frac{\sum c' b_i / \cos \alpha_i + \tan \phi' \sum W_i \cos \alpha_i - u b_i / \cos \alpha_i}{\sum W_i \sin \alpha_i}, \quad (1)$$

where u is pore water pressure ($u = h_w \gamma_w$), and other parameters are given in Fig. 5.

Slices method (seismic load state) for effective soil pressure

Parameters used in seismic slope stability analysis are shown in Fig. 6. Forces acting on the failure surface are:

- (a) weight of wedge, W
- (b) inertia force on the wedge, $k_h W$, where k_h is the average coefficient of horizontal acceleration, and
- (c) resisting force per unit area s , the shear strength of soil acting along failure surface ABC.

The FS with respect to strength is given by:

FS = resisting moment about O/overturning moment about O

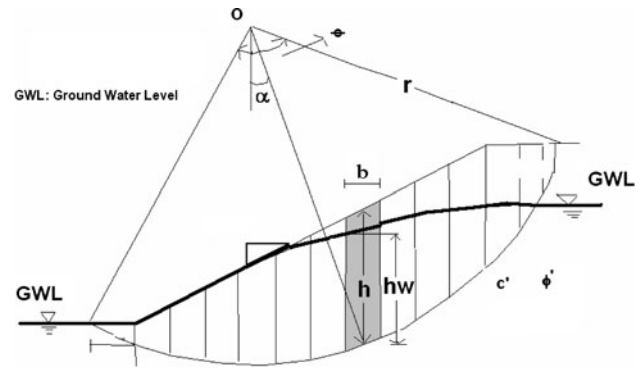


Fig. 5 Slope parameters for undrained shear strength parameters ϕ' , c'

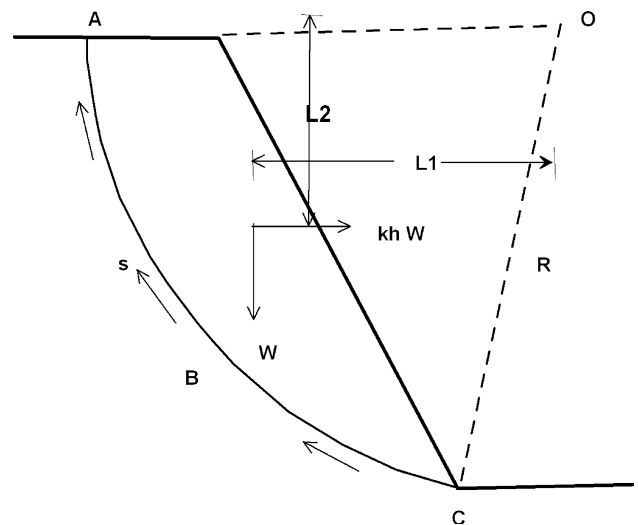


Fig. 6 Parameters for seismic slope stability [redrawn from Das (1993)]

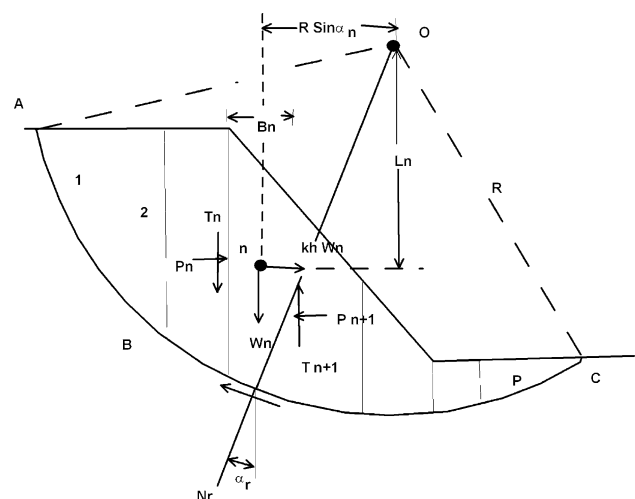


Fig. 7 Parameters for seismic slope stability analysis [redrawn from Das (1993)]

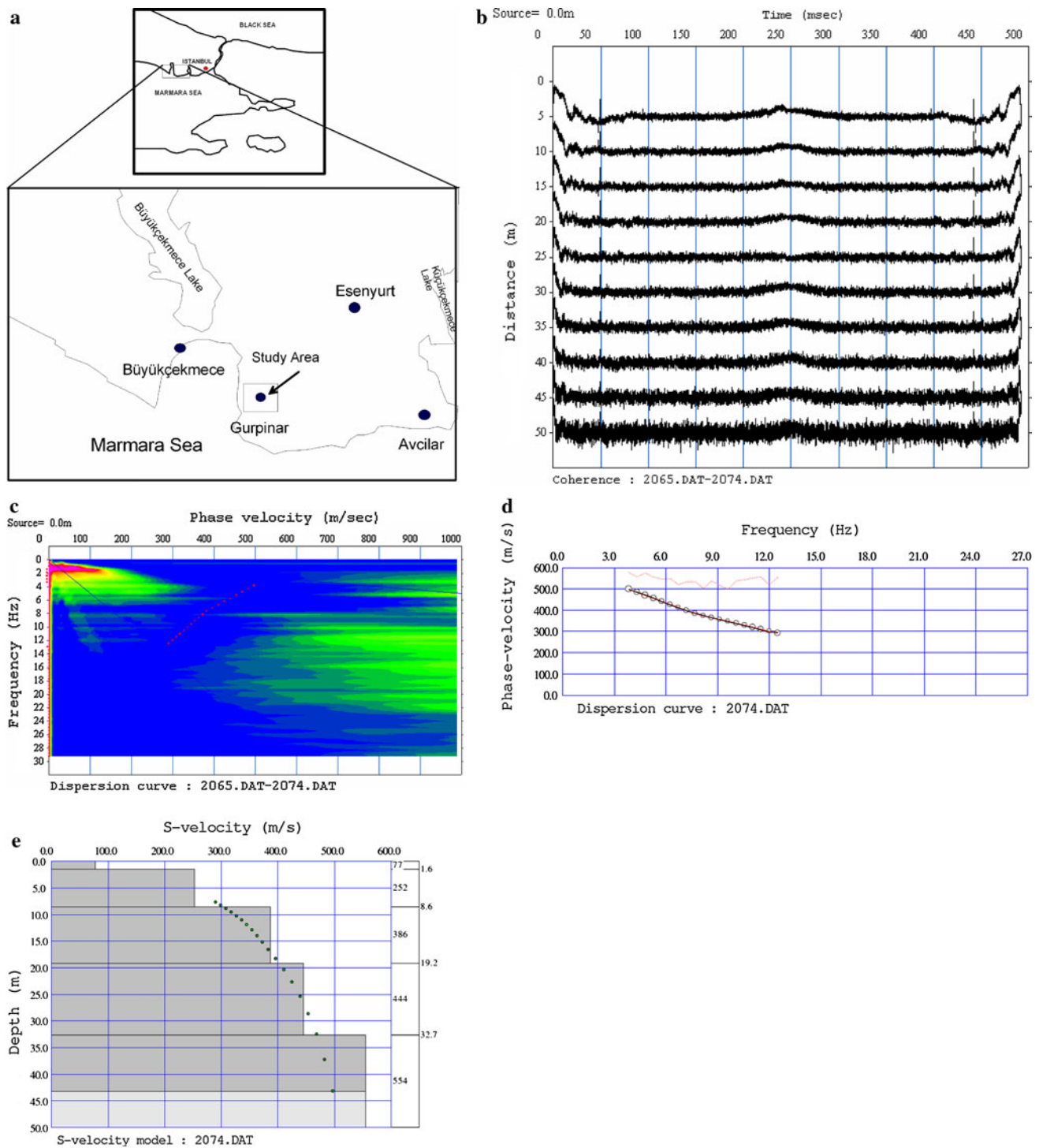


Fig. 8 **a** Location of study area. **b** Recorded data for the site. The active and passive source surface-wave records were taken in the field for both active and passive sources over 1–2 s. For the passive source, 6–7 records over about 35 s were taken. The data is obtained by overlaying these records. These figures are obtained from passive source data from the same area since the active source represents the

shallow parts of the study area? **c** Formation of the dispersion curve (site 36). Phase velocities and frequencies are determined from time-spatial surface-wave data using 2-D Fourier analysis. **d** Phase velocity–frequency curve for slope. **e** S-velocity versus depth of slope section. **f** (i) Borehole log in project area, 0–20 m. **f** (ii) Borehole log in project area, 21–40 m. **f** (iii) Borehole log in project area, 41–50 m

f (i)

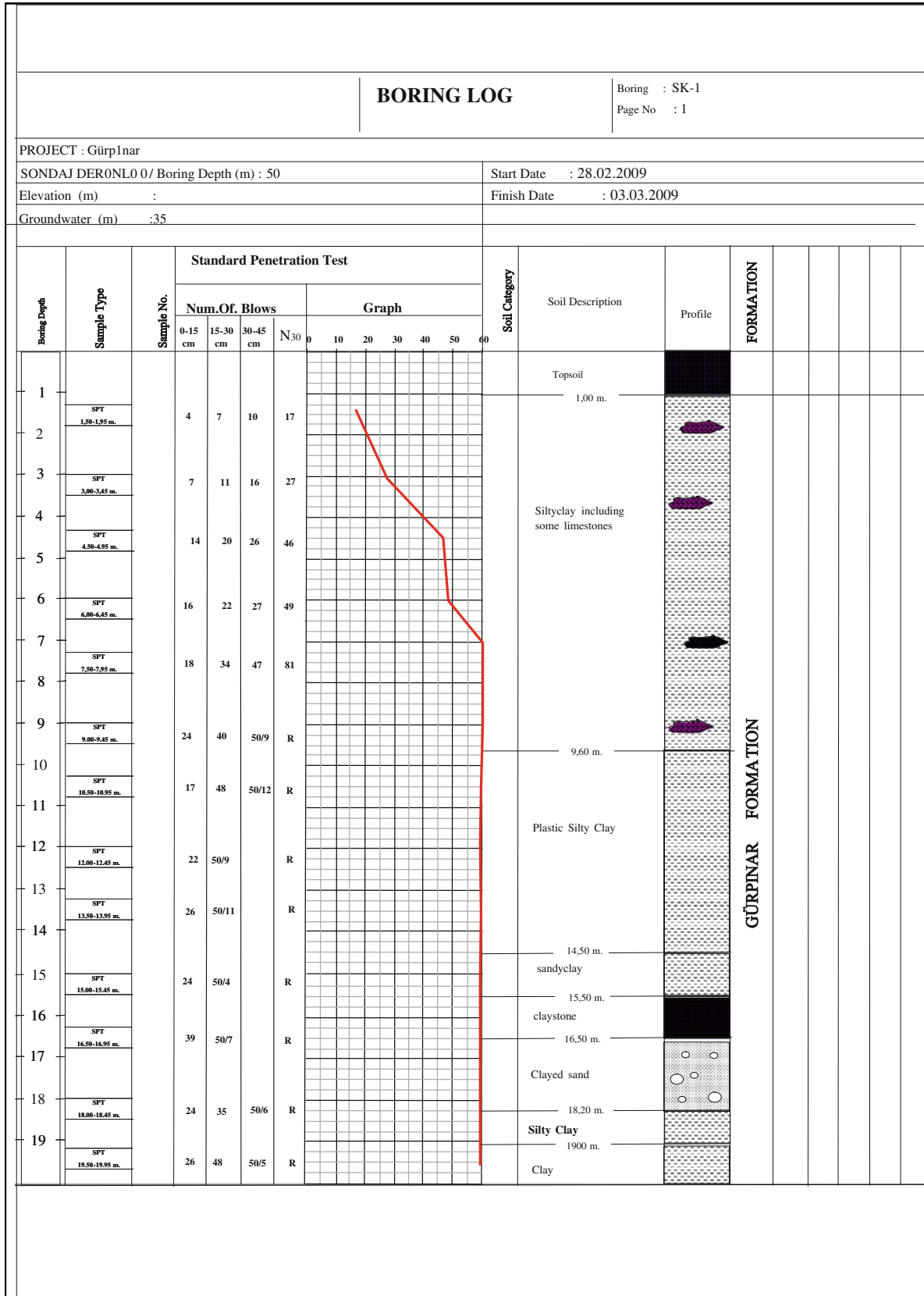


Fig. 8 continued

f (ii)

| BORING LOG | | | | | | | | | | | | | | | Boring : SK-1 | | | | |
|-----------------------|-------------------------|------------|---------------------------|----------|----------|-----------------|-------|----|----|--------------------------|----|----|---------------|------------------|---------------|-----------|--------------------------------|-------|----|
| | | | | | | | | | | | | | | | Page No : 2 | | | | |
| PROJECT : Gürpınar | | | | | | | | | | | | | | | | | | | |
| Boring Depth (m) : 50 | | | | | | | | | | Start Date : 28.02.2009 | | | | | | | | | |
| Elevation (m) : | | | | | | | | | | Finish Date : 03.03.2009 | | | | | | | | | |
| Groundwater (m) :35 | | | | | | | | | | | | | | | | | | | |
| Boring Depth | Sample Type | Sample No. | Standard Penetration Test | | | | | | | | | | Soil Category | Soil Description | Profile | FORMATION | TCR % (KAROT) Core Recovery | RQD % | |
| | | | Num.Of. Blows | | | | Graph | | | | | | | | | | | | |
| | | | 0-15 cm | 15-30 cm | 30-45 cm | N ₃₀ | 0 | 10 | 20 | 30 | 40 | 50 | | | | | | | 60 |
| 21 | SPT 21.00-21.45 m. | | 39 | 50/8 | | R | | | | | | | | | | | | | |
| 22 | | | | | | | | | | | | | | | | | | | |
| 23 | SPT 22.50-22.95 m. | | 44 | 50/4 | | R | | | | | | | | | | | | | |
| 24 | | | | | | | | | | | | | | | | | | | |
| 25 | SPT 24.00-24.45 m. | | 34 | 50/3 | | R | | | | | | | | | | | | | |
| 26 | | | | | | | | | | | | | | | | | | | |
| 27 | | | | | | | | | | | | | | | | | | | |
| 28 | SPT 27.0-27.45 m. | | 42 | 50/5 | | R | | | | | | | | | | | | | |
| 29 | | | | | | | | | | | | | | | | | | | |
| 30 | | | | | | | | | | | | | | | | | | | |
| 31 | SPT 30.0-30.45 m. | | 36 | 50/8 | | R | | | | | | | | | | | | | |
| 32 | | | | | | | | | | | | | | | | | | | |
| 33 | Karot 31.50-34.50 m. | | | | | | | | | | | | | | | | | | |
| 34 | SPT 33.0-33.45 m. | | 29 | 50/6 | | R | | | | | | | | | | | | | |
| 35 | | | | | | | | | | | | | | | | | | | |
| 36 | Karot 34.50-36.00 m. | | 24 | 50/4 | | R | | | | | | | | | | | | | |
| 37 | SPT 36.0-36.45 m. | | 10 | 17 | 45 | 62 | | | | | | | | | | | | | |
| 38 | Karot 36.50-37.00 m. | | | | | | | | | | | | | | | | | | |
| 39 | | | | | | | | | | | | | | | | | | | |

Fig. 8 continued

f (iii)

| BORING LOG | | | | | | | | | | | | | | Boring : SK-1 Page No : 3 | | | |
|-----------------------|-------------------------|------------|---------------------------|----------|----------|-----------------|--------------------------|----|----|---------------|------------------|---------|-----------|------------------------------|-------|----|----|
| PROJECT: Gürpınar | | | | | | | | | | | | | | | | | |
| Boring Depth (m) : 50 | | | | | | | Start Date : 28.02.2009 | | | | | | | | | | |
| Elevation (m) : | | | | | | | Finish Date : 03.03.2009 | | | | | | | | | | |
| Groundwater (m) :35 | | | | | | | | | | | | | | | | | |
| Boring Depth | Sample Type | Sample No. | Standard Penetration Test | | | | | | | Soil Category | Soil Description | Profile | FORMATION | TCR % Core Recovery | RQD % | | |
| | | | Num.Of. Blows | | | | Graph | | | | | | | | | | |
| | | | 0-15 cm | 15-30 cm | 30-45 cm | N ₃₀ | 0 | 10 | 20 | | | | | | | 30 | 40 |
| 41 | | | | | | | | | | | | | | | | | |
| 42 | Karot 41.50-43.50 m. | | | | | | | | | | | | | | | | 21 |
| 43 | | | | | | | | | | | | | | | | | |
| 44 | Karot 43.50-45.50 m. | | | | | | | | | | | | | | | | 36 |
| 45 | | | | | | | | | | | | | | | | | |
| 46 | Karot 45.50-47.50 m. | | | | | | | | | | | | | | | | 40 |
| 47 | | | | | | | | | | | | | | | | | |
| 48 | Karot 47.50-48.70 m. | | | | | | | | | | | | | | | | 43 |
| 49 | Karot 48.70-50.00 m. | | | | | | | | | | | | | | | | 61 |
| 50 | | | | | | | | | | | | | | | | | 47 |
| 51 | | | | | | | | | | | | | | | | | |
| 52 | | | | | | | | | | | | | | | | | |
| 53 | | | | | | | | | | | | | | | | | |
| 54 | | | | | | | | | | | | | | | | | |
| 55 | | | | | | | | | | | | | | | | | |
| 56 | | | | | | | | | | | | | | | | | |
| 57 | | | | | | | | | | | | | | | | | |
| 58 | | | | | | | | | | | | | | | | | |
| 59 | | | | | | | | | | | | | | | | | |
| | | | | | | | | | | | | | | | | | |
| | | | | | | | | | | | | | | | | | |

Fig. 8 continued

$$FS = s(ABC)R/WL_1 + k_h WL_2, \quad (2)$$

In the analysis of slope stability, it is assumed that the soil is homogeneous. However, in a given slope, layered soil can be encountered. This method is shown in Fig. 7.

The FS for this slope is given by (Das 1993):

$$FS = \frac{\sum_1^n P_n (cB_n \sec \alpha_n + W_n \cos \alpha_n \tan \phi)}{\sum_1^n P_n (W_n \sin \alpha_n + k_h W_n [L_n/R])}, \quad (3)$$

where α_n may be either positive or negative.

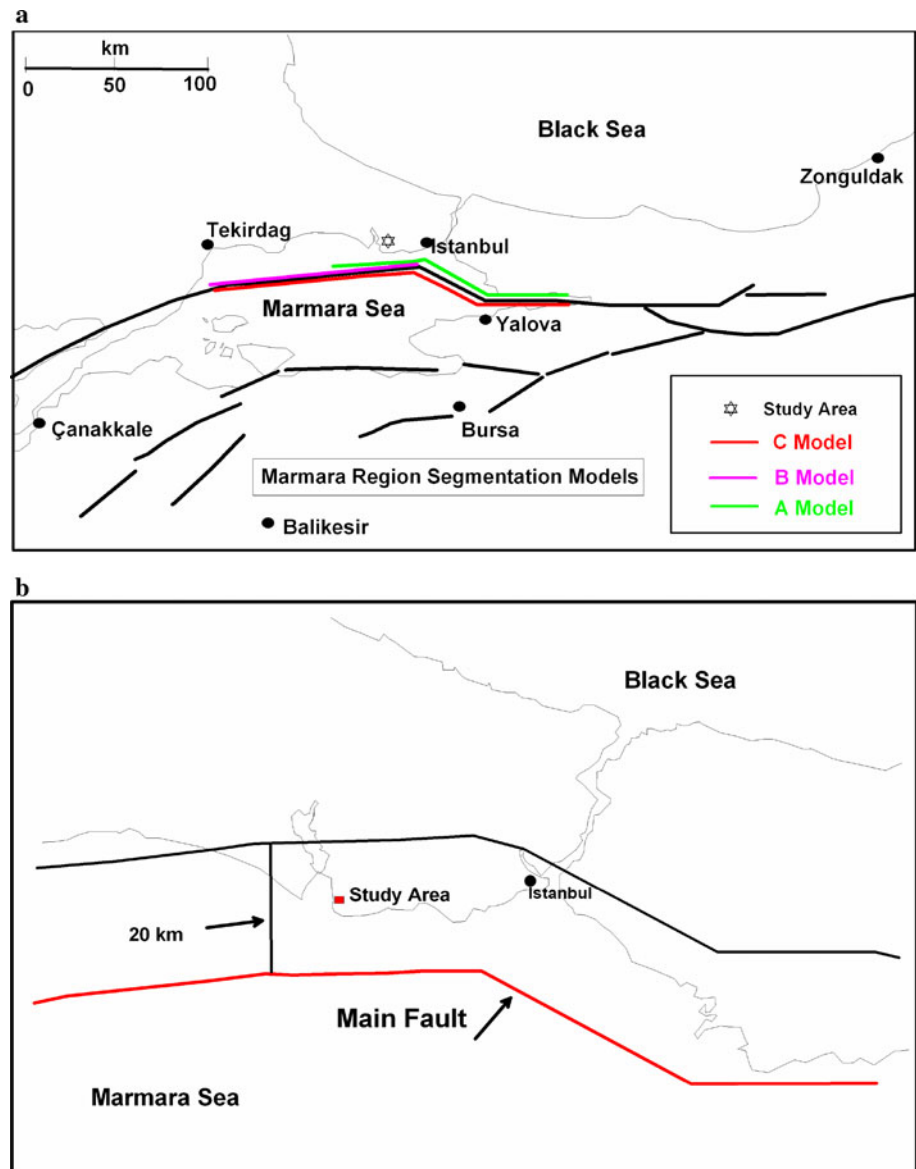
Analysis for study area

Study area: general geology and landslide features

The study area is shown in Fig. 8a. The general geology comprises the Trace Formation, Gurpinar Formation, Kırklareli Formation, Sazlıdere Formation, Bakırköy Formation, and Çukurçeşme Formation (Alparslan et al. 2006). The Gurpinar Formation is Miocene and upper Oligocene in age, and includes sandstone, limestone and claystone units, and several soil components, mainly clays.

Fig. 9 a Proposed models A, B, C for seismic hazard analysis in the Marmara region.

A approximately 119 km rupture length; B approximately 108 km rupture length; C approximately 174 km rupture length. b Seismogenetic fault for the study area



Landslides in this area are mainly observed in the fissured and over-consolidated plastic clays in Gurpinar Formation and are the rotational and retrogressive types (Dalgic 2005). The landslide morphology in many cases is not observable; due to construction work, the landslide morphology has been destroyed by landfill and excavations (Dalgic 2005; Dalgıç et al. 2009).

Geophysical and geotechnical studies

In the early 1980s spectral analysis of surface waves (SASW), a method of generating near-surface shear wave profiles, was carried out (Nazarian and Stokoe 1984). SASW uses the spectral analysis of ground roll generated

by an impulsive source and recorded by a pair of receivers. This method has been widely and effectively used in many geotechnical engineering projects (Stokoe et al. 1994). The necessity of recording repeated shots into multiple field deployments at a given site increases the time and labor requirements over a multichannel procedure. Multichannel analysis of surface waves (MASW) tries to overcome the few weaknesses of the SASW method (Park et al. 1999) and can deal with surface waves in the lower frequency range (e.g., 1–30 Hz) suitable for shallow-depth investigation work (e.g., a few meters to a few tens of meters) (Park et al. 2007).

Shear wave velocities and profiles were obtained by MASW, giving the phase velocity-dispersion curve and shear wave velocity profile for the upper 50 m of soil. An example of the application for the slope site is shown in Fig. 8b, which shows the records that were dependent on field conditions for different geophone intervals.

Linear arrays were applied in our study area. Processing the field data is carried out to obtain the phase velocities for different frequencies using Pickwin software. Finally the dispersion curve is obtained (Fig. 8c). SeisImager software combines Pickwin and Plotrefa software modules; SeisImager/SW-1D consists of the Pickwin and WaveEq modules; and SeisImager/SW-2D consists of the Pickwin, WaveEq, and GeoPlot modules. Surface Wave Analysis Wizard is not a separate module but automatically calls on specific subroutines from Pickwin, WaveEq, and GeoPlot to explain the analysis process. Passive (microtremor) and active source surface-wave data analyses:

- calculate phase velocity and automatically plot the dispersion curve,
- perform inversion to iteratively find the 1-D S-wave velocity (V_s) curve and 2-D V_s cross-section,
- allow active and passive source dispersion curves to be combined for a high-resolution result over all depths sampled,
- allow flexible geometry options to suit a wide range of site configurations and conditions,
- are based on robust methods: tau- p frequency domain, CMP cross-correlation for active source MASW; spatial autocorrelation (SPAC) for passive source microtremor array measurements (MAM),
- and include QC editing of velocity functions and velocity modeling.

During the field studies, seismic refraction data were also collected. The initial model obtained from this data

Table 1 Equations for rupture length and magnitude estimations

| Researcher | M (magnitude) | Magnitude Type |
|------------------------------|-----------------------------|----------------|
| Ambraseys and Zatopek (1968) | $M = 0.881 \log L + 5.62$ | Ms |
| Douglas and Ryall (1975) | $M = (\log L + 4.673)/0.9$ | Ms |
| Ezen (1981) | $M = (\log L + 2.19)/0.577$ | Ms |
| Matsuda (1977) | $M = (\log L + 2.9)/0.6$ | Ms |
| Toksoz et al. (1979) | $M = (\log L + 3.62)/0.78$ | Ms |
| Wells and Coppersmith (1994) | $M = 1.12 \log L + 5.16$ | Mw |
| Wells and Coppersmith (1994) | $M = 1.16 \log L + 5.08$ | Mw |

Table 2 Rupture length and magnitude estimations. Model A: approximately 120 km rupture length; Model B: approximately 108 km rupture length; Model C: approximately 174 km rupture length

| Researcher | M (magnitude) ranges for A model | M (magnitude) ranges for B model | M (magnitude) ranges for C model |
|------------------------------|------------------------------------|------------------------------------|------------------------------------|
| Ambraseys and Zatopek (1968) | 7.4 | 7.4 | 7.6 |
| Douglas and Ryall (1975) | 7.5 | 7.5 | 7.7 |
| Ezen (1981) | 7.4 | 7.3 | 7.7 |
| Toksoz et al. (1979) | 7.3 | 7.2 | 7.5 |
| Wells and Coppersmith (1994) | 7.5 | 7.4 | 7.7 |

Table 3 Number of earthquakes within about 100 km radius of the study area, calculated from Eq. (3)

| Magnitude ranges | $4.5 \leq M < 5.0$ | $5.0 \leq M < 5.5$ | $5.5 \leq M < 6.0$ | $6.0 \leq M < 6.5$ | $7.0 \leq M < 7.5$ |
|------------------|--------------------|--------------------|--------------------|--------------------|--------------------|
| Numbers | 31 | 12 | 7 | 1 | 1 |

was used in the initial model. By using both forward and inverse solutions algorithms, *S*-wave velocities are calculated and drawn depending on distance (Figs. 8d, e).

In this study, a Geometrics Smart Seis SE seismic instrument, geophone, and other seismic tools are used. Records were controlled in the field and, after making the necessary adjustments to obtain refraction data, soil structure were modeled by using Seis Imager 1D Pickwin/Surface Wave Analysis software.

In the study area, boreholes were logged to 50 m depth at nine locations; a typical drilling log is shown in Fig. 8f.

Seismic hazard analysis of study area

Seismic hazard analysis refers to the probability of occurrence per unit time of certain levels of ground motion caused by earthquakes (Erdik et al. 1999; Erdik and Durukal 2004). This analysis is often summarized by a seismic hazard graph of the annual probability of exceedance versus ground motion amplitude. Both deterministic and probabilistic seismic hazard analyses were used to evaluate the seismic hazard in the region. The potential earthquake source was taken to be the North Anatolian Fault in the Marmara Sea.

Deterministic seismic hazard analysis

Required input for deterministic hazard analysis is a designation of active faults or earthquake sources in the

Table 4 Probabilities of earthquake occurrence for region

| Magnitude | For <i>D</i> = 10 (years) probability (%) | For <i>D</i> = 50 (years) probability (%) | For <i>D</i> = 75 (years) probability (%) | For <i>D</i> = 100 (years) probability (%) |
|-----------|---|---|---|--|
| 5 | 92.4 | 100.0 | 100.0 | 100.0 |
| 5.5 | 67.7 | 99.6 | 100.0 | 100.0 |
| 6 | 39.0 | 91.6 | 97.5 | 99.3 |
| 6.5 | 19.4 | 66.1 | 80.3 | 88.5 |
| 7 | 9.0 | 37.7 | 50.8 | 61.2 |
| 7.6 | 4.1 | 18.7 | 26.7 | 33.9 |

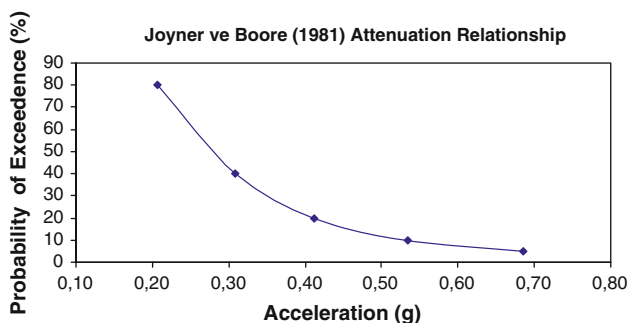


Fig. 10 Hazard curve for the region (Joyner and Boore (1981) attenuation model)

region. For the Marmara region (Fig. 9a, b), magnitudes were estimated for three models (A, B, and C) for seismic hazard analysis (JICA-IBB Report 2002):

- Model A: approximately 119 km rupture length;
- Model B: approximately 108 km rupture length; and
- Model C: approximately 174 km rupture length (Tables 1, 2).

Probabilistic seismic hazard analysis of region

Table 3 refers to earthquakes within about 100 km radius of the study area. Gutenberg-Richter recurrence relationships were determined from:

$$\log N = 3.0 - 0.71M. \tag{4}$$

The earthquake occurrence probabilities in Table 4 are obtained from:

$$R_m = 1 - e^{-N(M)D}, \tag{5}$$

where R_m is risk value (%); D is duration; $N(M)$ refers to the value of M used in Eq. (4).

The attenuation relationship was defined by two attenuation models: from a set of attenuation relationships, the design acceleration value for the city was calculated to be 0.41 g [Joyner and Boore (1981) model] and 0.4 g [Campbell (1997) model] with a 50-year exceedance probability of 20%. Finally, the hazard curve for the region was estimated (Fig. 10). Estimated acceleration values for magnitude 7.5 earthquakes are given in Table 5.

Table 5 Estimated acceleration values for 7.5 magnitude, 15 km epicentral distance (Δ , km) and 15 km focal depth (H , km)

| | |
|---------------------------------|------|
| Esteva (1970) | 0.24 |
| Donovan (1973) | 0.75 |
| Esteva and Villaverde (1973) | 0.61 |
| Donovan (1973) | 0.29 |
| Donovan (1973) | 0.30 |
| McGuire (1984) | 0.40 |
| Shah et al. (1975) | 0.55 |
| Oliveira (1974) | 0.24 |
| Joyner and Boore (1981) | 0.70 |
| Campbell (1981) | 0.24 |
| Campbell (1981) | 0.23 |
| Newmark and Roseblueth (1971) | 0.43 |
| Kanai (1966) | 0.55 |
| Esteva and Roseblueth (1964) | 0.48 |
| Fukushima et al. (1988) | 0.35 |
| Abrahamson and Litehiser (1989) | 0.34 |
| Campbell (1997) | 0.57 |
| Average acceleration (g) | 0.43 |

Fig. 11 **a** First model **b** second model **c** third model

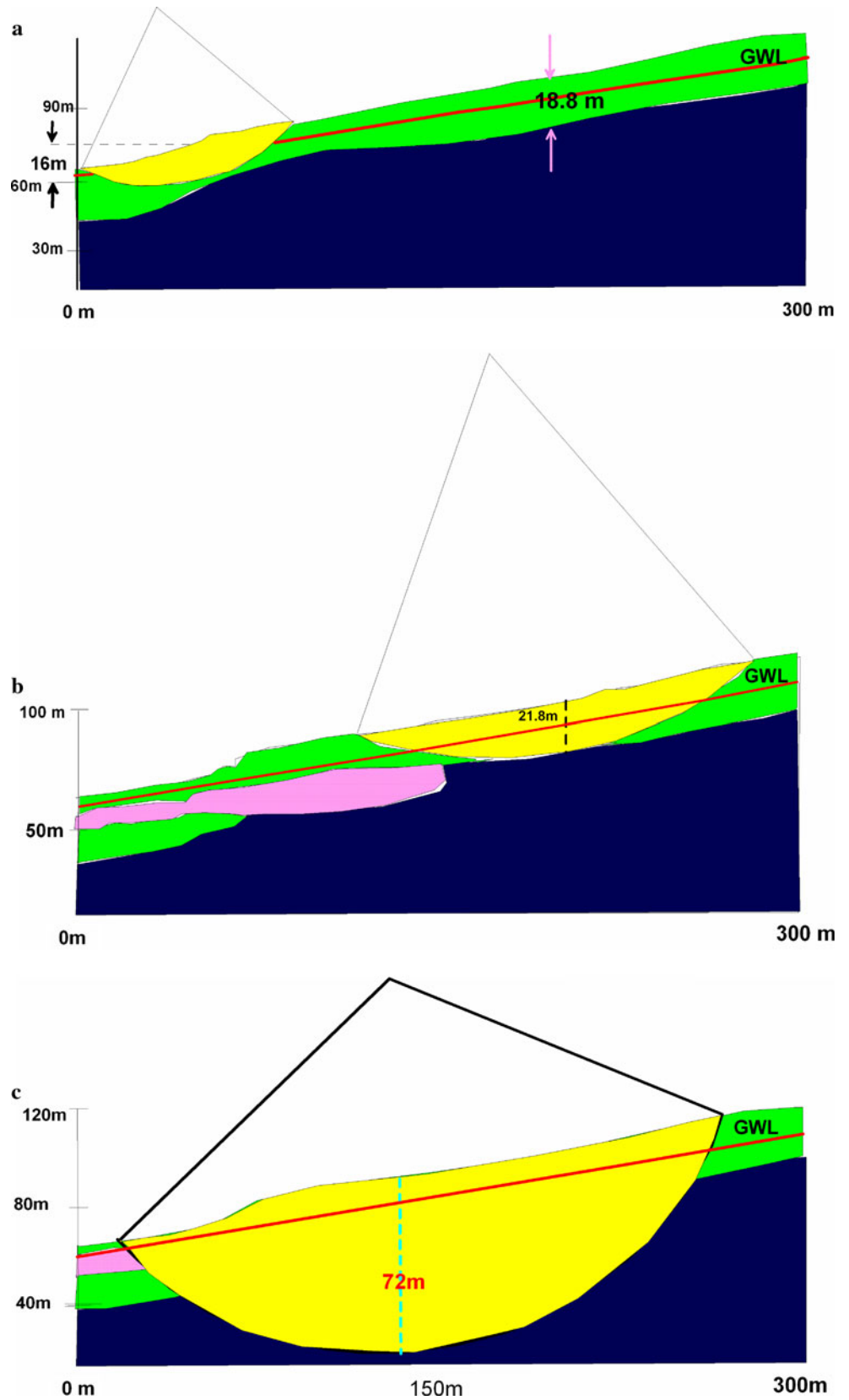


Table 6 Safety factor for static and dynamic conditions with geometrical and mechanical parameters for first slope model ($R = 73.70$ m)

| SF static | 2.5 | | | | | | |
|----------------------------------|---------|---------|--------|-------------------------------|----------|------------|---------|
| SF earthquake (for $k_h = 0.2$) | 1.2 | | | | | | |
| Slice no | b (m) | h (m) | hw (m) | γ (kN/m ³) | α | c' (kPa) | ϕ' |
| 1 | 7.1 | 3.3 | 0.1 | 19 | -25.0 | 23 | 14 |
| 2 | 7.1 | 6.6 | 3.3 | 19 | -20.0 | 23 | 14 |
| 3 | 7.1 | 7.9 | 4.6 | 19 | -15.0 | 23 | 14 |
| 4 | 7.1 | 10.6 | 6.6 | 19 | -10.0 | 23 | 14 |
| 5 | 7.1 | 13.2 | 7.3 | 19 | -3.0 | 23 | 14 |
| 6 | 7.1 | 14.5 | 7.3 | 19 | 3.0 | 23 | 14 |
| 7 | 7.1 | 16.6 | 8.6 | 19 | 10.0 | 23 | 14 |
| 8 | 7.1 | 17.2 | 11.9 | 19 | 15.0 | 23 | 14 |
| 9 | 7.1 | 16.5 | 9.9 | 19 | 20.0 | 23 | 14 |
| 10 | 7.1 | 13.2 | 7.9 | 19 | 28.0 | 23 | 14 |
| 11 | 7.1 | 11.9 | 4.6 | 19 | 33.0 | 23 | 14 |
| 12 | 7.1 | 8.6 | 3.3 | 19 | 38.0 | 23 | 14 |
| 13 | 7.1 | 6.6 | 0.0 | 19 | 45.0 | 23 | 14 |

The design acceleration coefficient, k_h was determined from:

$$k_h = 0.3(I + 1)A_0 \quad (5)$$

and/or

$$k_h = 0.2(I + 1)A_0, \quad (6)$$

where I is the structure importance factor ($1 \leq I \leq 1.5$), A_0 is the estimated earthquake acceleration (0.43 g). In this study, k_h coefficient was selected as 0.20 g.

The relationship between earthquake and slope failure is shown in Figs. 1, 2 and 3. For an epicentral distance of 15 km from the main fault in the study area, a minimum of magnitude 6.0 may trigger slope failure in the study area. For this reason, a detailed seismic slope stability analysis was carried out in the study area.

Detailed slope stability analysis for static and seismic conditions

In the study area, in situ SPT tests were carried out and laboratory samples were obtained from six boreholes (maximum depth 50.0 m) to determine soil classification and strength characteristics. Geophysical studies (seismic refraction and MASW) were also carried out for estimation of the structure and strength characteristics of the slope to 50.0 m depth. All field and laboratory data were used to predict the mechanical and structural (geometrical) behavior of the slope. Three soil slope models were considered.

The geometrical features and failure surface of the first, second, and third models are shown in Figs. 11a, b, and c. Analysis results are given in Tables 6, 7, 8, 9.

Table 7 Safety factor for static and dynamic conditions with geometrical and mechanical parameters for second slope model ($R = 169.40$ m)

| SF static | 1.5 | | | | | | |
|----------------------------------|---------|---------|--------|-------------------------------|----------|------|---------|
| SF earthquake (for $k_h = 0.2$) | 0.9 | | | | | | |
| Slice No | b (m) | h (m) | hw (m) | γ (kN/m ³) | α | c' | ϕ' |
| 1 | 13.7 | 3.8 | 0.0 | 19 | -17.0 | 23 | 14 |
| 2 | 13.7 | 10.2 | 0.0 | 19 | -13.0 | 23 | 14 |
| 3 | 13.7 | 14.8 | 3.8 | 19 | -8.0 | 23 | 14 |
| 4 | 13.7 | 16.6 | 6.4 | 19 | -5.0 | 23 | 14 |
| 5 | 13.7 | 19.2 | 6.4 | 19 | 1.0 | 23 | 14 |
| 6 | 13.7 | 19.2 | 6.4 | 19 | 6.0 | 23 | 14 |
| 7 | 13.7 | 21.8 | 7.6 | 19 | 10.0 | 23 | 14 |
| 8 | 13.7 | 19.2 | 7.6 | 19 | 15.0 | 23 | 14 |
| 9 | 13.7 | 17.9 | 7.6 | 19 | 20.0 | 23 | 14 |
| 10 | 13.7 | 14.0 | 5.1 | 19 | 25.0 | 23 | 14 |
| 11 | 13.7 | 12.8 | 1.6 | 19 | 28.0 | 23 | 14 |
| 12 | 13.7 | 10.2 | 0.0 | 19 | 35.0 | 23 | 14 |
| 13 | 6.9 | 3.8 | 0.0 | 19 | 39.0 | 23 | 14 |

Results and discussion

Matasovic (1991) has pointed out that the seismic stability of natural slopes is a subject about which much uncertainty still exists. The main problems associated with predicting slope behavior during and after earthquake motion are connected with the shear strength parameters of the material and the estimation of adequate seismic loading. In addition, both local topography and the presence of surface

Table 8 Safety factor for static and dynamic conditions with geometrical and mechanical parameters for third slope model ($R = 151.98$ m), assuming clay soil

| | | | | | | | |
|----------------------------------|---------|--------------------|--------|-------------------------------|-----------------------------|-----------------------------|---------|
| SPT(N) | 40 | Hara et al. (1971) | | Stroud (1974) minimum value | Stroud (1974) average value | Stroud (1974) maximum value | |
| Cohesion c_u (kPa) | 413 | 140 | | 175 | 260 | | |
| SF static | 2.5 | | | | | | |
| SF earthquake (for $k_h = 0.2$) | 1.2 | | | | | | |
| Slice no | b (m) | h (m) | hw (m) | γ (kN/m ³) | α | c' | ϕ' |
| 1 | 24.2 | 18.3 | 12.2 | 18 | -37.0 | 175 | 14 |
| 2 | 24.2 | 34.2 | 30.5 | 18 | -28.0 | 175 | 14 |
| 3 | 24.2 | 57.3 | 45.1 | 18 | -18.0 | 175 | 14 |
| 4 | 24.2 | 67.0 | 56.1 | 18 | -8.0 | 175 | 14 |
| 5 | 24.2 | 70.7 | 59.7 | 18 | 1.0 | 175 | 14 |
| 6 | 24.2 | 73.2 | 68.3 | 18 | 7.0 | 175 | 14 |
| 7 | 24.2 | 70.7 | 58.6 | 18 | 18.0 | 175 | 14 |
| 8 | 24.2 | 62.2 | 52.5 | 18 | 28.0 | 175 | 14 |
| 9 | 24.2 | 56.1 | 39.0 | 18 | 40.0 | 175 | 14 |
| 10 | 24.2 | 31.7 | 18.3 | 18 | 53.0 | 175 | 14 |
| 11 | 6.1 | 7.3 | 0.0 | 18 | 63.0 | 175 | 14 |

Table 9 Safety factor for static and dynamic conditions with geometrical and mechanical parameters for third slope model ($R = 151.98$ m), assuming sandy soil

| | | | | | | | |
|----------------------------------|---------|---------|--------|-------------------------------|----------|---------|--|
| SF static | 2.5 | | | | | | |
| SF earthquake (for $k_h = 0.2$) | 1.2 | | | | | | |
| Slice No | b (m) | h (m) | hw (m) | γ (kN/m ³) | α | ϕ' | |
| 1 | 24.2 | 18.3 | 12.2 | 18 | -37.0 | 38 | |
| 2 | 24.2 | 34.2 | 30.5 | 18 | -28.0 | 38 | |
| 3 | 24.2 | 57.3 | 45.1 | 18 | -18.0 | 38 | |
| 4 | 24.2 | 67.0 | 56.1 | 18 | -8.0 | 38 | |
| 5 | 24.2 | 70.7 | 59.7 | 18 | 1.0 | 38 | |
| 6 | 24.2 | 73.2 | 68.3 | 18 | 7.0 | 38 | |
| 7 | 24.2 | 70.7 | 58.6 | 18 | 18.0 | 38 | |
| 8 | 24.2 | 62.2 | 52.5 | 18 | 28.0 | 38 | |
| 9 | 24.2 | 56.1 | 39.0 | 18 | 40.0 | 38 | |
| 10 | 24.2 | 31.7 | 18.3 | 18 | 53.0 | 38 | |
| 11 | 6.1 | 7.3 | 0.0 | 18 | 63.0 | 38 | |

layers are likely to have caused the observed amplification effects that are thought to have contributed to the triggering of some of the hundreds of landslides related to this seismic event (Bourdeau et al. 2004).

The stability of a slope during or after a seismic event was studied using the pseudostatic approach which estimates the stability of a slope under dynamic loading, incorporating the dynamic safety factor. Cherubini et al. (2004) have suggested that this approach is not able to account for either the seismic displacements of the slope or

the influence of the duration and the time variation of the seismic shock acceleration over the slope displacements. In the first phase of the present study, seismic hazard analysis of the study region was carried out by deterministic and probabilistic means to determine the level of ground motion that triggers slope failure. Relationships between the magnitude of an earthquake causing slope failures and their distance from a fault or an epicenter were also examined in the study area context. The main seismogenic source of the region is the North Anatolian Fault Zone in the Marmara Sea.

Both static and seismic slope stability analyses were carried out and the safety factor of the slope was determined. While no stability problem was found for the static case, unsafe seismic safety factors of 0.8 and 0.9 were obtained. Slope improvement is proposed for the study area.

References

Abrahamson NA, Litehiser JJ (1989) Attenuation of vertical peak acceleration. *BSSA* 79(3):549–580

Alparslan E, Yüce H, Erkan B, Inan S, Ergintav S, Saatçılar R (2006) Multi-criteria analysis of landslide susceptibility İn: The Area Between Büyükçekmece And Küçükçekmece Lakes Of İstanbul City Using Remote Sensing And Gis, 4th Gis Days İn Türkiye, Sep 13–16, 2006/Fatih University/Istanbul-Türkiye

Ambraseys N, Zatopek A (1968) The Varto, Antolia, earthquake of 19 August 1966. *Bull Seism Soc Amer* 58:47–102

Bourdeau C, Havenith H, Fleurisson J, Grandjean G (2004) Numerical modelling of seismic slope stability, in engineering geology for infrastructure planning in Europe. Springer, Heidelberg

- Campbell KW (1981) Near source attenuation of peak horizontal acceleration. *Bull Seis Soc Am* 71(6):2039–2070
- Campbell KW (1997) Empirical near-source attenuation relationships for horizontal and vertical components of peak ground acceleration, peak ground velocity, and pseudo-absolute acceleration response spectra. *Seismol Res Lett* 68(1):154–179
- Cherubini C, Santoro F, Vessia G (2004) Hazard assessment in dynamic slope stability analysis. In: Brebbia CA (ed) *Risk analysis IV*. Wessex Institute of Technology, UK
- Dalgıç S (2005) İstanbul ili, Büyükçekmece ilçesi, yerleşime uygun olmayan alanların jeolojik jeoteknik değerlendirme raporu, İÜ, Araştırma ve Yardım Vakfı
- Dalgıç S, Turgut M, Kuşku I, Coşkun C, Coşgun T (2009) The effect of soil and rock conditions on Construction Foundation on the European Side of İstanbul. *Appl Earth Sci J Kocaeli University*, 2:47–70
- Das BM (1993) *Principles of soil dynamics*. HWS Publications, USA
- Donovan NC (1973) A statistical evaluation of strong motion data including the February 9, 1971 San Fernando earthquake, World Conference on Earthquake Engineering, V, Rome, Proceedings, v. 2, paper 155, International Association for Earthquake Engineering, Istituto di Scienza e Techn? ca delle. Construzioni Politecnico di Milano, Piazza da Leonardo da Vinci, 32, 20133 Milano, Italia
- Douglas BM, Ryall A (1975) Return periods of rock accelerations in western Nevada. *BSSA* 65:1599–1611
- Erdik M, Durukal E (2004) Strong ground motion. In: Ansal A (ed) *Recent advances in earthquake geotechnical engineering and microzonation*. Kluwer Academic Publishers, The Netherlands
- Erdik M, Alpaz Biro Y, Onur T, Sesetyan K, Birgoren G (1999) Assessment of earthquake hazard in Turkey and neighboring regions. *Annali di Geofisica* 42:1125–1138
- Esteva L (1970) Seismic risk and seismic design decisions, in seismic design for nuclear power plants. MIT Pres, Cambridge
- Esteva L, Rosenblueth E (1964) Spectra of Earthquakes at moderate and large distances. *Soc Mex De Ing Seismica*, Mexico 11
- Esteva L, Villaverde R (1973) Seismic risk, design spectra and structural reliability. Proceedings 5th World Conference on Earthquake Engineering., Rome 2, 2586–2596
- Ezen Ü (1981) Earthquake source parameters related to magnitude along the North-Anatolian Fault zone. *Bull Int Inst Seism Earth Eng (Japan)* 19:33–55
- Fukushima Y, Tanaka T, Kataoka S (1988) A new attenuation relationship for peak ground acceleration derived from strong motion accelerograms. Proceedings of IX WCEE, Tokyo
- ISSMFE (1993) *Manual for zonation on seismic geotechnical hazards*, Japanese Soc Soil Mech Found Eng, Maruei Co., Ltd., Japan
- JICA-IBB Report (2002) *The study on a disaster prevention/mitigation basic plan in İstanbul including seismic microzonation in the Republic of Turkey*, Final Report, Main Report, December 2002, Pacific Consultants International, OYO Corporation, Japan International Cooperation Agency (JICA), İstanbul Metropolitan Municipality (IMM), 729 p
- Joyner WB, Boore DM (1981) Peak horizontal acceleration and velocity from strong motion records, including records from the 1979 Imperial Valley, California, earthquake. *Bull Seis Soc Am* 71(6):2011–2038
- Hara A, Ohata T, Niwa M (1971) Shear modulus and shear strength of cohesive soils. *Soils Found* 14(3):1–12
- Kanai K, Hisrano K, Yoshizawa S, Asada T (1966) Observation of strong earthquake motion in Matsushiro area, part 1. *Bull Earth Res Inst, Univ Tokyo* 44:1269–1296 (In Japanese)
- Matasovic N (1991) Selection of method for seismic slope stability analysis, Proceedings, Second International Conference on Recent Advances in Geotechnical Earthquake Engineering and Soil Dynamics, Paper no: 7.20
- Matsuda T (1977) Estimation of future destructive earthquakes from active faults on land in Japan. *J Phys Earth* 25:S251–S260
- McGuire RK (1984) *Ground Motion Estimation In Regions With Few Data*. VIII WCEE, vol 2. San Francisco, pp 327–334
- Nazarian S, Stokoe IKH (1984) In-Situ shear wave velocities from spectral analysis of surface waves, Proceedings 8th Conference on Earthquake Engineering—S.Francisco, vol 3. Prentice-Hall, pp 31–38
- Newmark NM, Rosenblueth E (1971) *Fundamentals of earthquake engineering*. Prentice Hall, New Jersey
- Oliveira CS (1974) *Seismic risk analysis*, report no. EERC. 74-I, University of California, Berkeley
- Park CB, Miller RD, Xia J (1999) Multichannel analysis of surface waves (MASW). *Geophysics* 64:800–808
- Park CB, Miller RD, Xia J, Ivanov J (2007) Multichannel analysis of surface waves (MASW)—active and passive methods. *The Leading Edge* 2007:60–64
- Shah HC, Huang MJ, Kremidjian AS, Zstutty TC (1984) A study of seismic risk for Nicaragua Part I. Report 11, The John A. Blume Earthquake Engineering Center, Stanford University, Stanford, California
- Stokoe KH II, Wright GW, James AB, Jose MR (1994) Characterization of geotechnical sites by SASW method. In: Woods RD (ed) *Geophysical characterization of sites*. Oxford Pub, Oxford
- Stroud MA (1974) The standard penetration test in insensitive clays and soft rocks. Proceedings of European seminar on penetration testing, Stockholm, pp 367–375
- Tamura T (1978) An analysis of the relation ship between the areal distribution of earthquake-induced landslides and the earthquake magnitude. *Geogr Rev Japan* 51–58:662–672
- Toksoz MN, Shakal AF, Michael AJ (1979) Space time migration of earth-quakes along the North Anatolian fault zone and seismic gaps. *Pure Appl Geophys* 117:1258–1270
- Wells DL, Coppersmith KJ (1994) New empirical relationships among magnitude, rupture length, rupturewidth and surface displacement. *Bull Seis Soc Am* 84:974–1002